Comptes Rendus
Géoscience — Sciences de la Planète
Supplementary material to the article available at:
https://doi.org/10.5802/crgeos.214

Supplementary material: Bubble connectivity in experimentally-sheared crystal-bearing silicic melts

Camille Daffos [a], Caroline Martel [*, a], Laurent Arbaret [a] and Rémi Champallier [a]

[a] Institut des Sciences de la Terre d'Orléans (ISTO), Univ. Orléans, CNRS, BRGM, UMR 7327, Orléans, France

E-mails: camille.daffos@univ-orleans.fr (C. Daffos), caroline.martel@cnrs-orleans.fr (C. Martel), laurent.arbaret@univ-orleans.fr (L. Arbaret), remi.champallier@cnrs-orleans.fr (R. Champallier)

1. Methods

The experiments consisted in three main phases: (i) synthesis of a crystal-bearing hydrated glass by melt hydration in an internally-heated pressure vessel and mixing of the obtained hydrated glass with plagioclase crystals, (ii) H_2O-bubble formation by decompression in the Paterson-type apparatus, and (iii) subsequent deformation in simple shear of the three-phase magma.

1.1. *Experimental methods*

1.1.1. *Synthesis of crystal-bearing hydrated glasses*

The anhydrous starting glass is a haplogranite (HPG8, prepared by Schott AG, Germany) with the eutectic composition of the quartz–albite–orthoclase system [Holtz et al., 1992; composition in wt%: 78.6 SiO_2, 12.5 Al_2O_3, 4.6 Na_2O, 4.2 K_2O). About 10 g of the powdered (<90 μm) anhydrous HPG8 glass was mixed with either about 1 g or 0.5 g deionized H_2O, and sealed in 20-mm diameter and 30-mm long Au capsules. The HPG8 hydrations were performed in internally-heated pressure vessels pressurized with argon (at ISTO) at T of 750 and 950 °C and P of 400 MPa (for the capsules containing 1 g H_2O) and P of 170 MPa (for the capsules containing 0.5 g H_2O). The H_2O contents introduced in the capsules were enough to ensure H_2O solubilities at P of 400 MPa and 170 MPa (950 °C) according to the H_2O solubility model of Newman and Lowenstern [2002], i.e. 9.6 and 5.0 wt% H_2O, respectively. Hydration durations were 48 to 96 h, which is long enough to homogenize H_2O by diffusion in the HPG8 glass powder, according to Zhang and Behrens [2000]. The samples were isobarically quenched by shutting down the furnace, in order to avoid H_2O exsolution from the melt. The recovered hydrated HPG8 glasses were ground in an agate mechanical grinder to obtain a ~20-μm grain size powder, to which plagioclase crystals were added. We purchased commercially a plagioclase block of labradorite (anorthite content of 50 to 70 mol%) whose composition was tested for chemical resistance at the contact of the HPG8 hydrated melt under the elected run conditions. The labradorite block was reduced into pieces using a high-voltage pulsed power fragmentation apparatus (Selfrag, at BRGM, Orléans, France). The main advantage of the Selfrag is to crush rocks at the grain joints, so that we were expecting more or less elongated bits,

* Corresponding author.

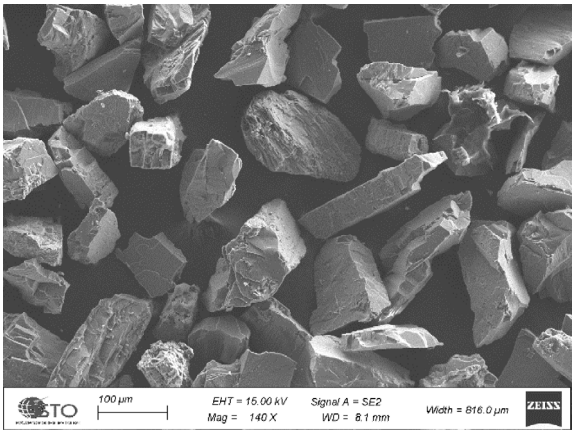

Supplementary Figure S1. The 50–90 µm fraction size of the plagioclase crystals.

i.e. resembling the natural plagioclase shapes. The recovered fragments were sieved to 50–90 µm (Supplementary Figure S1), before manual mixing with the hydrated HPG8 glass powder following different weight proportions. Very minor amounts of crystals other than plagioclase (presumably Fe–Ti oxides and pyroxenes) have been found in the fragments, likely coming from mineral inclusions trapped in the labradorite block. Recalculated to volume proportions using a 2.7 density for labradorite, four series based on their crystal contents ($\Phi_{c\_melt\_3D}$) have been chosen: 0, 21, 50, and 70 vol%.

1.1.2. *Synthesis of bubble-bearing magmas*

About 1.6–2.0 g of the crystal-glass mixtures were sealed in 14-mm diameter and 12-mm long Cu capsules in order to prevent H_2O loss. The capsules were sandwiched between alumina spacers, alumina and zirconia pistons, and the whole assembly was coated by an iron jacket (Figure 1b). The sample column was placed at the hot spot of the internal Mo-furnace of the gas-medium (argon) Paterson rig [Paterson and Olgaard, 2000; Australian Scientific Instruments Pty Ltd, at ISTO; Figure 1a]. The samples were (i) pressurized to 240 MPa, (ii) heated to 850 °C (pressure will reach 300 MPa) at a rate of 10 °C/min and maintained during 15 min for thermal equilibration, then (iv) decompressed to 50 MPa within 9 to 20 min in order to generate H_2O bubble nucleation, (v) maintained for 45 min to let bubbles grow, and (vi) cooled to 650 °C (crystal-free samples) or 750 °C (crystal-bearing samples), in order to allow further deformation without inconvenient jacket breakage, followed by a 15-min dwell for thermal equilibration (Figure 1c). In the Paterson rig, all samples were decompressed from 300 MPa (maximum pressure allowed in the Paterson rig), so that the samples pre-hydrated at 400 MPa (~9.6 wt% H_2O) nucleated between 300 and 50 MPa [possibly during annealing at 300 MPa, although the high supersaturations >100 MPa required for homogeneous nucleation in silica-rich melts would favour nucleation at pressure below 300 MPa; Mourtada-Bonnefoi and Laporte, 2002]. The samples hydrated to 5.0 wt% H_2O nucleated at pressure between 170 and 50 MPa.

1.1.3. *Torsion experiments*

Keeping the experimental setup as it was after decompression, deformation in right-lateral simple shear was carried out at T of 650 °C (crystal-free samples) or 750 °C, P of 50 MPa, and shear rate γ_r of 2×10^{-4} s^{-1}. Torsion durations were 1 or 2 h, which led to bulk finite shear γ of 1 and 2, respectively, [see Paterson and Olgaard, 2000, for γ calculation]; note that in torsion, the sample centre experiences zero torque and, therefore, zero strain; both strain and strain rate increase radially toward the sample exterior. Temperature, pressure, shear stress and angular displacement were live recorded on a computer. The experiment was ended by relaxing the stress, followed by an isobaric quench (shut of the furnace while maintaining 50 MPa confining pressure) at a rate of ~40 °C/min from 750 to 200 °C. According to Mader et al. [2013], the relaxation time (λ) of a bubble writes as: $\lambda = (a \times \eta_{melt})/\sigma$, where a is the bubble's equivalent spherical radius, η_{melt} is the viscosity of the hydrated melt, and σ is the surface tension at the bubble-liquid interface. Considering a = 10 and 100 µm (from the sample analyses), $\eta_{melt} = 10^{6.3}$ Pa·s [HPG8 melt with 2.9 wt% H_2O at 50 MPa and 750 °C; Hess and Dingwell, 1996], and σ = 0.2 N/m at 50 MPa [Bagdassarov et al., 2000], λ would be about 2 and 17 min, respectively. At 700 °C, $\eta_{melt} = 10^{6.9}$ Pa·s and λ becomes 7 and 66 min for bubble radius of 10 and 100 µm, respectively. During quenching, about 42 s are spent between 750 and 700 °C, so that we infer that in our experiments, the small 10-µm radius bubbles fully relaxed (returned to sphericity), whereas the larger 100-µm radius bubbles experienced limited relaxation during quenching. After experiment,

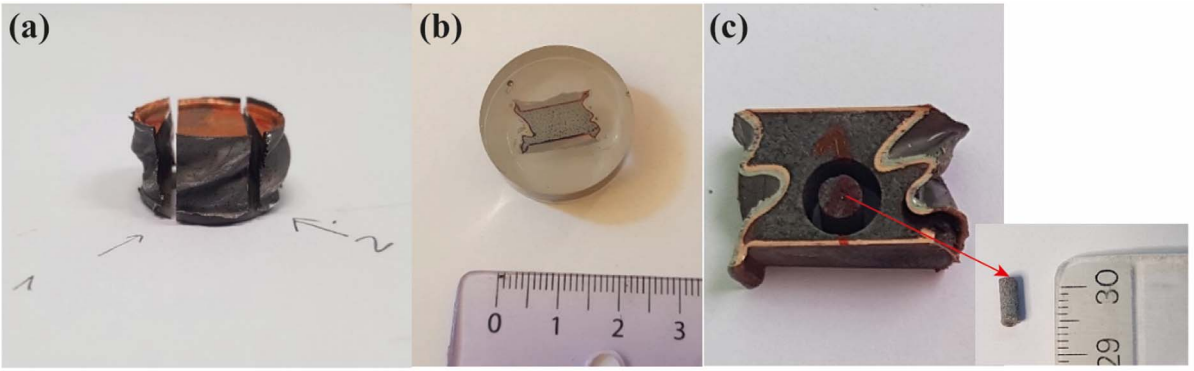

Supplementary Figure S2. After run sample preparation for analyses. (a) Cutting, (b) polish section with one outer piece of the sample, and (c) bore of a 3-mm cylinder in the middle piece.

the sample column was extracted from the vessel and the extent of deformation was verified by the progress of the pen-markers between the non-deformed (piston) and deformed (sample) parts. The iron jacket was removed to release the Cu-capsule containing the sample. Note that shear stress could not be determined in-situ during deformation due to the low viscosity (high temperature) of the samples, so that bulk viscosity could not be measured.

1.2. *Analytical methods*

1.2.1. *Microstructural analysis*

After experiment, the Cu capsule containing the sample was cut following two sections parallel to the shear plane, in order to expose their longitudinal tangential surfaces, which represent the planes of maximum shear strain [Paterson and Olgaard, 2000] (Supplementary Figure S2a). One of the two sections was placed in epoxy, polished, and carbon coated for two-dimensional (2D) observations using a scanning electron microscope (SEM; Merlin Compact Zeiss at ISTO) (Supplementary Figure S2b).

The sample polished sections being about 5–10 mm long by 10–15 mm wide and often showing microtextural heterogeneities, the sample analysis was performed by processing 5 to 10 thumbnail images that covered the whole section. The SEM images were segmented using the SPO2003 image-processing software [Launeau and Robin, 1996, Launeau and Cruden, 1998], in order to determine the average 2D bubble and crystal contents (accuracy of ±3 area% determined on repeated measurements), bubble and crystal sizes, shapes, and orientations (following the method of intercepts; [Launeau and Robin, 1996], and bubble and crystal number densities, as follows:

- Crystal-free bubble content: $\Phi_{b\_melt\_2D}$ = (bubble area)/(bubble area + glass area) × 100;
- 2D-bulk porosity: $\Phi_{b\_bulk\_2D}$ = (bubble area)/(bubble area + glass area + crystal area) × 100;
- 2D-bubble-free crystal content: $\Phi_{c\_melt\_2D}$ = (crystal area)/(crystal area + glass area) × 100;
- 2D-bulk crystal content: $\Phi_{c\_bulk\_2D}$ = (crystal area)/(bubble area + glass area + crystal area) × 100;
- 2D-bulk glass content: $\Phi_{g\_bulk\_2D}$ = glass area/(bubble area + glass area + crystal area) × 100;
- Crystal-free areal bubble number density: BND = (number of bubbles)/(glass area).
- Bubble-free areal crystal number density: CND = (number of crystals)/(glass area).
- Bubble long and short axes; bubble eccentricity: R = (long axis)/(short axis); the radius (a) equivalent to the bubble surface; bubble orientation to the horizontal (θ_b).

1.2.2. *X-ray Computed Tomography (XCT)*

After the removal of the two longitudinal tangential sections for the 2D analysis, the sample rest was bored perpendicularly to the shear plane (0 strain

in centre; Supplementary Figure S2c) in order to get an oriented 3-mm core sample for three-dimensional (3D) analysis using XCT (Phoenix NanoTOM at ISTO). The XCT images were reconstructed using a Phoenix 3D software with a voxel resolution of 1.4-µm side. A qualitative analysis of the whole core sample was performed in order to segment the glass+crystal matrix, the isolated bubbles, and the bubbles connected to the outside of the core sample, using the commercial software VGStudio Max. Smaller sample volumes (cubes of 600 and 1400-µm side) were defined to qualify bubble size and spatial distribution, as well as to quantify the 3D bulk porosity ($\Phi_{b\_bulk\_3D}$) and the volume content of bubbles connected to the sample border ($\Phi_{b\_connect\_3D}$), using the commercial software Blob3D. The porosity measurements, $\Phi_{b\_bulk\_3D}$ and $\Phi_{b\_connect\_3D}$, were determined with an accuracy of ±3 vol%. Because the small size of the experimental samples precludes porosity 3D measurement iterations, the assumption made here is that the volumes on which the measurements have been made are representative of the whole experimental sample.

1.2.3. *Glass H_2O contents*

The H_2O contents of the starting hydrated glasses were checked using an elemental analyser (ThermoFlash2000 at ISTO), given with a precision of ±0.15 wt%. The results confirmed the H_2O solubility data from [Newman and Lowenstern, 2002], i.e. H_2O contents of 9 to 10 wt% for the 400-MPa hydrations and ~5 wt% for the 170-MPa hydrations. As the elemental analyser is a destructive method (sample pyrolyze), the H_2O contents of the residual glasses from the run products were analysed using an electron microprobe (EMP; Cameca SX Five at ISTO) following the "by-difference" method of Devine et al. [1995], and using HPG8 glass standards with known H_2O contents [samples from Martel et al., 2000]. The analysed elements were Si, Al, Ca, Na, K, with alkalis analysed first, in order to minimize loss under the electron beam. The EMP conditions were set to an acceleration voltage of 15 kV, a beam current of 6 nA, peak/background counting times of 10/5 s for all elements, and a defocussed beam of 10 × 10 µm size. The analytical errors on major elements were calculated at ~1% (relative) for SiO_2, Al_2O_3 and CaO, and 5% for Na_2O and K_2O, and ±0.7 wt% on the H_2O content.

Some of the residual glasses were double-checked by microRaman spectroscopy. The Andor Shamrock 500i spectrometer is coupled with a Nikon ECLIPSE Ni-U microscope uses a long working distance Nikon objective (100×, numerical aperture of 0.8), which allows lateral resolution of 1–2 µm^2. A monochromatic 532 nm Coherent Genesis MX SLM laser was used as exciting source (output laser power was set to 300 mW). The 1200 lines/mm grating was used, providing two spectral windows spanning 200 to 1500 cm^{-1} (silicate network) and 2895 to 3800 cm^{-1} (OH stretching region). For each analysis, the acquisition time was 60 s. In order to determine H_2O content, the HPG8 glass standards were measured in the same analytical conditions as the samples. The Raman spectra were proceeded following the method of Behrens et al. [2006].

1.3. *Calculations*

1.3.1. *Gas fraction*

The gas fraction equation of Jaupart and Allegre [1991] calculates the gas volume (α_{melt}) resulting from degassing of a H_2O-saturated melt in closed-system. The equation writes as follows:

$$\alpha_{melt} = 1/\{1 + \rho_{gas}/[(Cw_i - Cw_f) \times \rho_{liq}]\} \times 100 \quad (1)$$

where ρ_{gas} is the H_2O density at T and final P calculated after Burnham et al. [1969], ρ_{liq} is the melt density taken as 2400 kg/m^3, Cw_i and Cw_f are the H_2O solubilities at initial and final pressures, respectively, calculated after Newman and Lowenstern [2002]. The uncertainty associated with the α_{melt} calculation mostly depends on the precision of the melt H_2O contents (Cw_i and Cw_f). Assuming an uncertainty of ±0.7 wt% on the EMP "by-difference" H_2O measurements suggests uncertainties of ±3 vol% on α_{melt} calculations.

1.3.2. *Bulk viscosity*

The bulk viscosity (η_{bulk}) of our samples were calculated using the Equation (3.2) of Truby et al. [2015] that gives the relative viscosity (η_r, with $\eta_r = \eta_{bulk}/\eta_{melt}$) of a three-phase suspension of bubbles and crystals in a Newtonian liquid undergoing steady flow. The model adopts an "effective medium" approach in which the bubbly liquid is treated as a continuous medium which suspends the crystals. The model is valid for a low bubble capillary number (Ca)

regime. Ca describes the ratio of the viscous stress to the restoring stress and writes as follows: $Ca = (\eta_{\text{melt}} \times \gamma_r)/(\sigma/a)$, where a is the bubble's equivalent spherical radius. For γ_r of 2×10^{-4} s^{-1}, bubble radius of 10 and 100 µm, σ of 0.2 N/m [Bagdassarov et al., 2000], and η_{melt} of $10^{6.3}$ Pa·s (HPG8 liquid with 2.9 wt% H_2O at 750 °C; [Hess and Dingwell, 1996], Ca is ~0.02 and 0.2, respectively, which satisfies the low Ca regime ($Ca < 1$) required for the viscosity calculation. The equation writes:

$$\eta_r = (1 - \Phi_{\text{b\_melt\_3D}}/100)^{-1} \times (1 - \Phi_{\text{c\_bulk\_3D}}/\Phi_{\text{max}})^{-2} \quad (2)$$

where Φ_{max} is the particle maximum packing of 66 vol% [Truby et al., 2015].

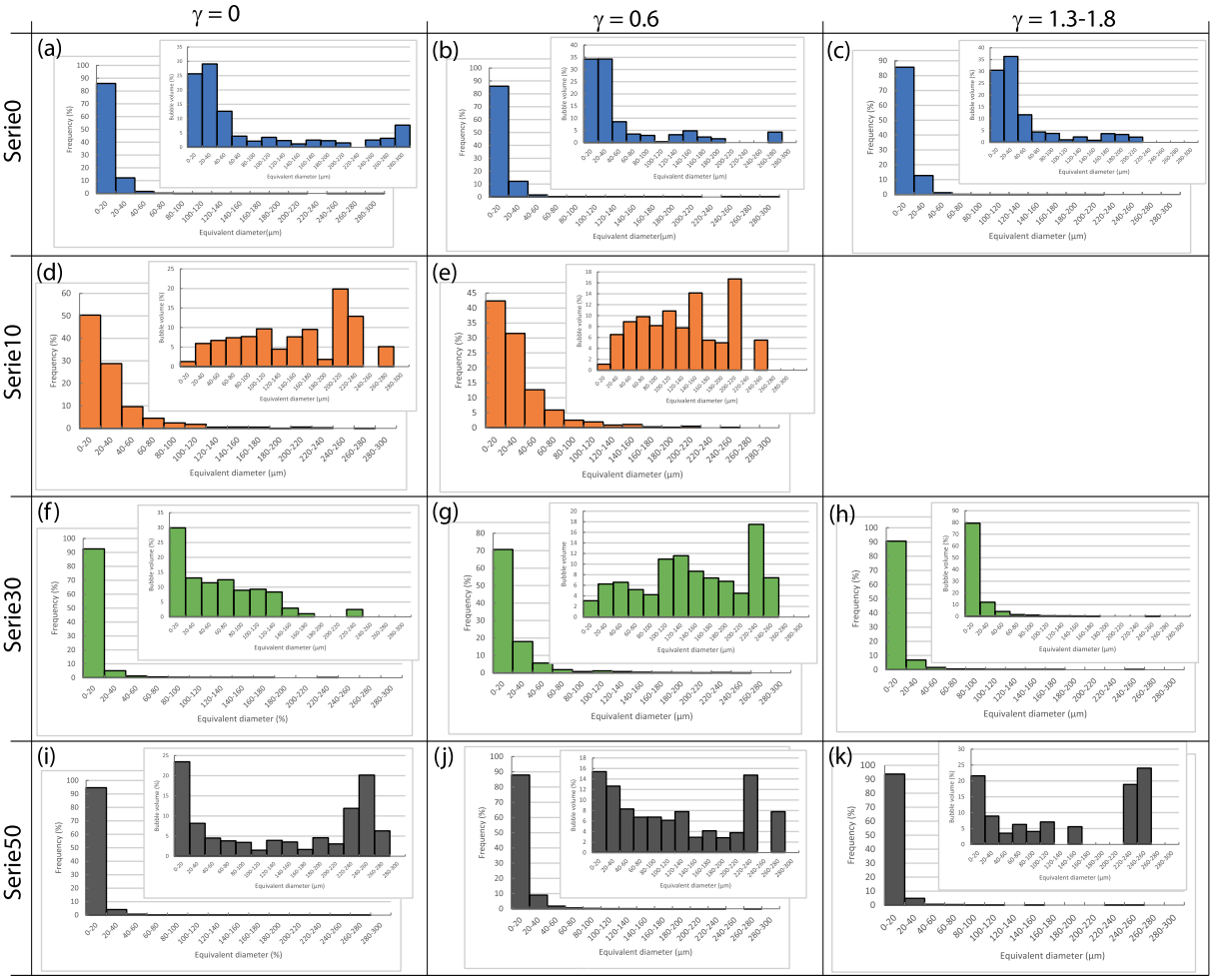

Supplementary Figure S3. 3D bubble size distributions.

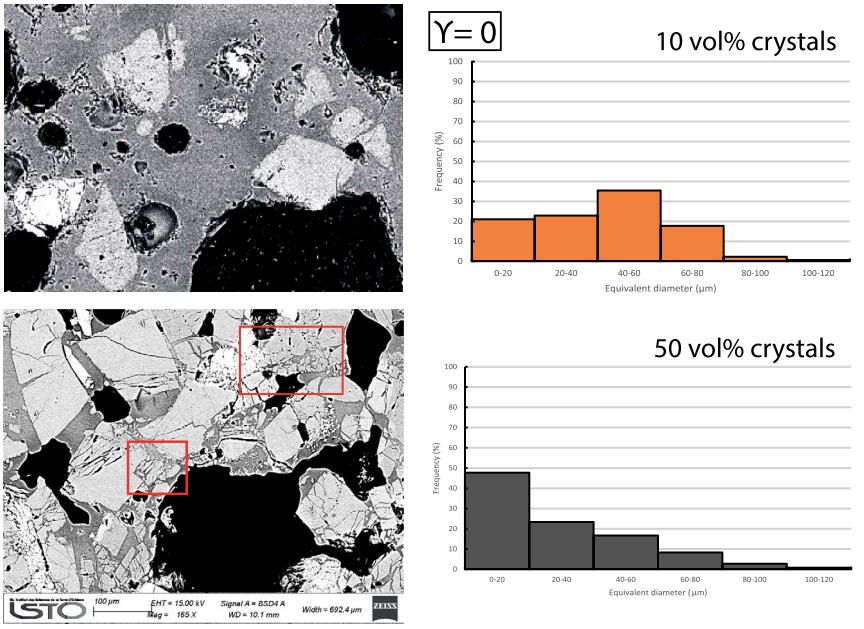

Supplementary Figure S4. Crystal breakage. The red squares highlight crystal breakage in the undeformed ($\gamma = 0$) sample containing 50 vol% crystals (bottom left) and associated crystal size histogram showing a large population of 0–20 µm diameter crystals (bottom right), in contrast to non-broken crystals in the undeformed sample containing 10 vol% crystals (upper left; same scale bar) associated to a lower frequency of 0–20 µm crystals (upper right).

References

Bagdassarov, N. S., Dorfman, A., and Dingwell, D. B. (2000). Effect of alkalis, phosphorus, and water on the surface tension of haplogranite melt. *Am. Mineral.*, 85, 33–40.

Behrens, H., Roux, J., Neuville, D. R., and Siemann, M. (2006). Quantification of dissolved H_2O in silicate glasses using confocal microRaman spectroscopy. *Chem. Geol.*, 229, 96–112.

Burnham, C. W., Holloway, J. R., and Davis, N. F. (1969). Thermodynamic properties of water to 1000 °C and 10,000 bars. *Geol. Soc. Am. Spec. Papers*, 132, 1–96.

Devine, J. D., Gardner, J. E., Brack, H. P., Layne, G. D., and Rutherford, M. J. (1995). Comparison of microanalytical methods for estimating H_2O contents of silicic volcanic glasses. *Am. Mineral.*, 80, 319–328.

Holtz, F., Behrens, H., Dingwell, D. B., and Taylor, R. P. (1992). Water solubility in aluminosilicate melts of haplogranite composition at 2 kbar. *Chem. Geol.*, 96(3–4), 289–302.

Martel, C., Dingwell, D. B., Spieler, O., Pichavant, M., and Wilke, M. (2000). Fragmentation of foamed silicic melts: an experimental study. *Earth Planet. Sci. Lett.*, 178, 47–58.

Zhang, Y. and Behrens, H. (2000). H_2O diffusion in rhyolitic melts and glasses. *Chem. Geol.*, 169, 243–262.